

***Ab initio* molecular-dynamics simulations of the structural properties of liquid $\text{In}_{20}\text{Sn}_{80}$ in the temperature range 798–1193 K**

G. Zhao, C. S. Liu,* and Z. G. Zhu

Key Laboratory of Materials Physics, Institute of Solid State Physics, Chinese Academy of Sciences, Post Office Box 1129, Hefei 230031, People's Republic of China

(Received 21 July 2005; published 9 January 2006)

Ab initio molecular dynamics simulations on a liquid $\text{In}_{20}\text{Sn}_{80}$ alloy have been carried out at six different temperatures from 798 to 1193 K. We have studied the temperature-dependent structure properties, including binding energy, volume, pair correlation function, coordination number, structure factor, and bond-angle distribution function. The dynamical and electronic properties have also been studied. The calculated pair correlation function is in agreement with experimental data. A shoulder was reproduced in the high wave number side of the first peak in the calculated structure factor and the angle distribution function shows two peaks located at about 53° and 102° , implying the existence of the residual directional bonds of Sn atoms in a liquid $\text{In}_{20}\text{Sn}_{80}$ alloy. The coordination number of a Sn atom and the first-peak height of the calculated structure factor decrease more sharply in a low-temperature region from 798 K to 986 K than that in a high-temperature region from 986 to 1193 K, so there is a noticeable bend at around 986 K in the curves of both coordination number versus temperature, and peak height versus temperature. In the high temperature region, the most prevalent atomic bonded pairs are the 1311 type, whereas in the low temperature region, the most prevalent atomic bonded pairs are the 1551 type. In the middle temperature region (929–986 K), with decreasing temperature, there seems to exist a steplike increase for 1551-, 1541-, 1441-, and 1431-type pairs and a steplike decrease for 1201-, 1311-, 1321-, and 1422-type pairs. However, the analysis based on the two-state model and the additional calculation at 963 K show that the change in local atomic structures is continuous, indicating that the abnormal structure change that happened in liquid $\text{In}_{20}\text{Sn}_{80}$ is not of first order.

DOI: [10.1103/PhysRevB.73.024201](https://doi.org/10.1103/PhysRevB.73.024201)

PACS number(s): 61.20.Ja, 61.25.Mv, 71.15.Pd

I. INTRODUCTION

The accurate structural information of liquid is important for the exact theoretical analysis of physicochemical properties; however, compared to the well-defined crystalline structure, understanding the liquid structure has been a challenge in material science and condensed matter physics. In crystals, first-order phase transitions induced by pressure and/or temperature constitute a class of phenomena which has been thoroughly studied both experimentally and theoretically. At the same time, in liquids, can there be first-order phase transitions when the pressure and/or temperature changes? A widely accepted conventional view is that the liquid structure varies gradually with temperature and/or pressure from the melting point to the critical point. However, in recent years, more and more experimental and theoretical evidence suggests that the pressure-induced liquid-liquid phase transitions, characterized by two different densities related to different atomic configurations, happen in some one-component liquids, including H_2O , SiO_2 , P, Si, Se, C, S, Cs.^{1–14} For liquid P, Katayama *et al.*⁶ succeeded in observing the process of the transformation from a less dense to a denser liquid including the coexistence of the two phases by *in situ* x-ray diffraction measurements. In a supercooled state of $\text{Al}_2\text{O}_3\text{-Y}_2\text{O}_3$, Aasland and Mcmillan¹⁵ directly observed with optical microscopy the coexistence of two glassy liquids, which have completely the same composition but different density. However, in most cases, the existence of the liquid-liquid phase transition has been concluded from the indirect evidences. At the same time, there exists the controversy on

the liquid-liquid phase transition. For example, recently Wu *et al.*¹⁶ reported the results of first-principles molecular dynamics simulations showing no evidence of liquid-liquid phase transition in C, in the same temperature and pressure range where such a transition was found using empirical calculations.¹⁰ Although there have been a number of examples suggesting liquid-liquid phase transition, it has not been clarified how universal such a transition is or what is the condition for it.

Recently, with the revised internal friction method, x-ray diffraction, and differential thermal analysis (DTA) or differential scanning calorimetry (DSC), Zu *et al.* have suggested that, at hundreds of degree above the liquidus, a temperature-dependent discontinuous structural change might occur at ambient pressure in some binary liquids, such as PbSn, PbBi, InSn, and InBi.^{17,18} They presented the following evidence: (i) There is a notable peak in the curve of internal friction (Q^{-1}) as a function of temperature, and the features of this peak are in agreement with those exhibited during solid-solid phase transformations verified by previous investigators. (ii) A thermal absorption peak occurs in the DTA curve at the corresponding temperature range. (iii) The coordination number and mean nearest-neighbor distance, derived from the pair distribution functions, undergo an abnormal minimum. Surprisingly, such a structural transition does not fall into any other up-to-date recognized structural changes of liquids. Therefore, no doubt, it is necessary to further confirm it by understanding the microscopic atomic structure of these liquid alloys.

For understanding this counterintuitive liquid-structure change in $\text{In}_{20}\text{Sn}_{80}$ we have performed a quantitative analysis

based on the results of x-ray diffraction in our previous paper.¹⁹ The quantitative estimation of the viscosity (η) and the excess entropy (S) at seven different temperatures shows that there is a valley of viscosity in the η - T curve and a valley of excess entropy in the S - T curve, which are consistent with the internal-friction peak in the Q^{-1} - T curve and the exothermic peak in the DSC curve, respectively. The decomposition of S into two parts $S(1)$ and $S(2)$ clearly tells us that the atomic bonds vary twice and the microstructures transform twice in temperature range from 300 °C to 900 °C for liquid $\text{In}_{20}\text{Sn}_{80}$.

The development of *ab initio* molecular dynamics simulations makes it possible to study the atomic and electronic structure of liquid metals and alloys from the first-principles perspective. Over the past two decades, *ab initio* simulations have been performed on many liquids, giving much useful information about microscopic structure of liquid metals and alloys.^{20–26} In the present work, by *ab initio* molecular dynamics simulations we mainly investigate the temperature-dependent structural properties of a liquid $\text{In}_{20}\text{Sn}_{80}$ alloy at six different temperatures from 798 to 1193 K, in hope of theoretically confirming this counterintuitive behavior as mentioned above and obtaining some detailed microscopic structural information on liquid $\text{In}_{20}\text{Sn}_{80}$. The paper is organized as follows: in Sec. II, we describe the method of our simulations, the results of our simulations and the corresponding discussion are reported in Sec. III, and a short summary is given in Sec. IV.

II. COMPUTATIONAL METHODS

Our simulations were performed within the framework of the density function theory, with the local density approximation (LDA) to the exchange-correlation energy, and the valence electron-ion interaction was modeled by the projector augmented wave (PAW) potential,^{27,28} as implemented in the Vienna *Ab initio* Simulation Package (VASP).²⁹ $5s^2$ plus $5p^1$ states for In and $5s^2$ plus $5p^2$ states for Sn are treated as valence electrons. The system, which contains 64 Sn and 16 In atoms, was put in a simple cubic box with periodical boundary conditions. The Γ point was used to sample the Brillouin zone of the supercell. The electronic wave functions were expanded in the plane wave basis set, with an energy cutoff of 150 eV. Our microcanonical ensemble simulations have been performed at 798, 873, 929, 986, 1073, and 1193 K. The temperature-dependent box size was adjusted to make the variation of the internal pressure within 5 kbar at different temperatures. We believe such a small pressure variation will not bring significant errors for the comparison of structural properties at different temperatures. The Verlet algorithm was used to integrate Newton's equations of motion and the time step of ion motion was 4 fs. The Kohn-Sham energy functional was minimized by the preconditioned conjugate-gradient method.

The initial atomic configuration adopted was a random distribution of 80 atoms on the grid, which was constructed by dividing the supercell into $5 \times 5 \times 5$ square segments. After a microcanonical simulation for more than 8 ps, we got a liquid with a very high temperature. Gradually decreasing

the temperature of the hot liquid and adjusting the box size, we got a liquid with 798 K, at which the structure of the liquid was simulated and calculated. To get a higher temperature sample, we simply scale the velocities of atoms and the box size. At each temperature, the physical quantities of interest were obtained by averaging over 16 ps after the initial equilibration taking 8 ps. In order to estimate finite-size effects, we compare the results of structural properties with those obtained in a larger system of 120 atoms at 1193 K (see the figures below). They show the finite-size effects on the structural properties are expected to be small. The result of diffusion coefficient in the system of 120 atoms at 1193 K is 27% larger than that calculated in the system of 80 atoms. A similar result of diffusion coefficient in liquid Sn was reported by Itami *et al.*²²

III. RESULTS AND DISCUSSIONS

In Fig. 1, we present the calculated temperature-dependent binding energy and volume of the simulation cell at different temperatures for liquid $\text{In}_{20}\text{Sn}_{80}$. Apparently, the total binding energy decreases monotonically with the increase of the temperature and the volume can be approximately considered to have a linear relationship with temperature. It is well known that, at conditions below the critical point, the thermal expansion coefficient of liquid at constant pressure is approximately expressed as the following:

$$B_{\text{liquid}} = \frac{1}{V} \left(\frac{\partial V}{\partial T} \right)_P, \quad (1)$$

where B_{liquid} is the thermal expansion coefficient of liquid. The linear fit, as shown by the solid line in Fig. 1(b), yields a value of B_{liquid} of $1.085 \times 10^{-4} \text{ K}^{-1}$ at 900 K, which is comparable to that of pure liquid Sn ($9.991 \times 10^{-5} \text{ K}^{-1}$ at 900 K),³⁰ indicating that the volume of the simulation cell at each temperature is valid in our simulations on liquid $\text{In}_{20}\text{Sn}_{80}$. In addition, as can be seen from Fig. 1(b) by the dotted line, the thermal expansion coefficient of a region at high temperatures may be larger than that at relative low temperatures.

In the physics of fluids, the pair correlation function is an important physical quantity because it is directly measurable and, in principle, various properties of liquid materials can be estimated from the pair correlation function when coupled with an appropriate theory. In a two-component alloy, the total pair correlation function $g(r)$ is obtained by weighting the partial pair functions $g_{ij}(r)$ with the neutron scattering length,

$$g(r) = \sum_{i=1}^2 \sum_{j=1}^2 \frac{c_i c_j b_i b_j}{(c_1 b_1 + c_2 b_2)^2} g_{ij}(r), \quad (2)$$

where the neutron scattering lengths are $b_m = 4.065$ and $b_{\text{Sn}} = 6.225$;³¹ c_i and c_j are their number concentrations, respectively. $g_{ij}(r)$ is calculated by the following definition:

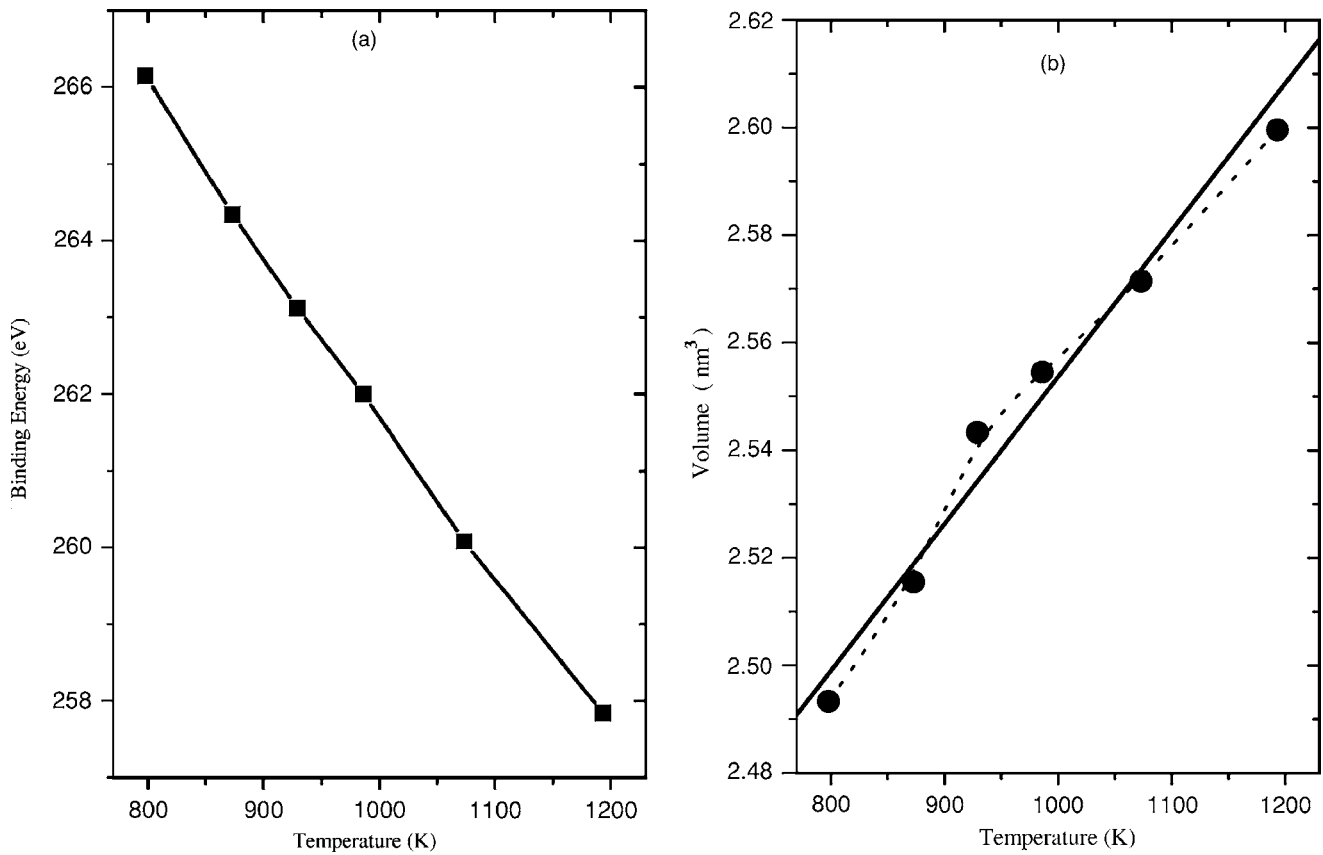


FIG. 1. Calculated properties of a liquid In₂₀Sn₈₀ alloy at different temperatures: (a) total binding energy for 80 atoms (64 Sn+16 In); (b) the volume of the simulation cell, the dotted line is a guide to the eye and the solid line is a curve fit obtained assuming a linear behavior.

$$g_{ij}(r) = \frac{1}{\rho_0 c_i c_j N} \left\langle \sum_i \sum_{j \neq i} \delta(\vec{r} - \vec{r}_{ij}) \right\rangle, \quad (3)$$

where ρ_0 is the average number density of the liquid, r_{ij} is the interatomic distance between atom i and j . Using the atomic coordinates from the molecular dynamics simulations, the total pair correlation functions of liquid In₂₀Sn₈₀, shown in Fig. 2(a), were calculated at six different temperatures ranging from 798 to 1193 K. As can be seen from Fig. 2(a), the characteristic feature of $g(r)$, i.e., large value or “flat shape” between the first peak position and the second one, and an asymmetry of the first peak, were reproduced in our simulations. But no obvious shoulder appears at the right side of the first peak. The first peak position of the total pair correlation function is around 0.313 nm, which is in good agreement with the experiment value 0.315 nm at 923 K.¹⁷ As can also be seen, the positions of the first and the second peaks are not sensitive to temperature, but the heights of them decrease with the increase of temperature. The partial pair functions $g_{Sn-Sn}(r)$, $g_{Sn-In}(r)$, and $g_{In-In}(r)$ were also calculated according to Eq. (3). The partial pair correlation functions between Sn atoms at different temperatures are plotted in Fig. 2(b). The first peak position of $g_{Sn-Sn}(r)$ is around 0.31 nm, which is slightly longer than that of pure liquid Sn (0.30 nm),²² and almost invariable with the variation of temperature. The heights of the first and the second peaks decrease with increasing temperature. The partial pair

correlation functions between Sn and In atoms are shown in Fig. 2(c). The first peak position of $g_{Sn-In}(r)$ is around 0.315 nm and there is almost no shift with temperature. The height of the first peak decreases with the increase of temperature and the same to that of the second one. The partial pair correlation functions between In atoms at different temperatures are also shown in Fig. 2(d). Because of the relatively small number of In atoms, the statistics for the $g_{In-In}(r)$ are not good, but we can see a maximum around 0.315 nm, which is close to the experimental value 0.31 nm for pure liquid In. In addition, as shown in Figs. 2(a)–2(d) the comparison of results between 80-atom and 120-atom systems indicates that the finite-size effect is much smaller.

According to the partial pair correlation functions given above, the average coordination numbers can be obtained by the integration of the $g_{ij}(r)$ to its first minimum,

$$N_{ij} = \int_0^{R_{cutoff}} 4\pi r^2 \rho_j g_{ij}(r) dr, \quad (4)$$

where $\rho_j = \rho_0 c_j$ is the partial number density of the atom j . Here, the cutoff distance R_{cutoff} is taken to be 0.44 nm, corresponding to the position of the first minimum of the pair correlation functions. Figure 3 plots the average coordination number of a Sn atom ($N_{Sn} = N_{Sn-Sn} + N_{Sn-In}$) as a function of temperature. Apparently, the average coordination number of a Sn atom decreases monotonically with the increase of the

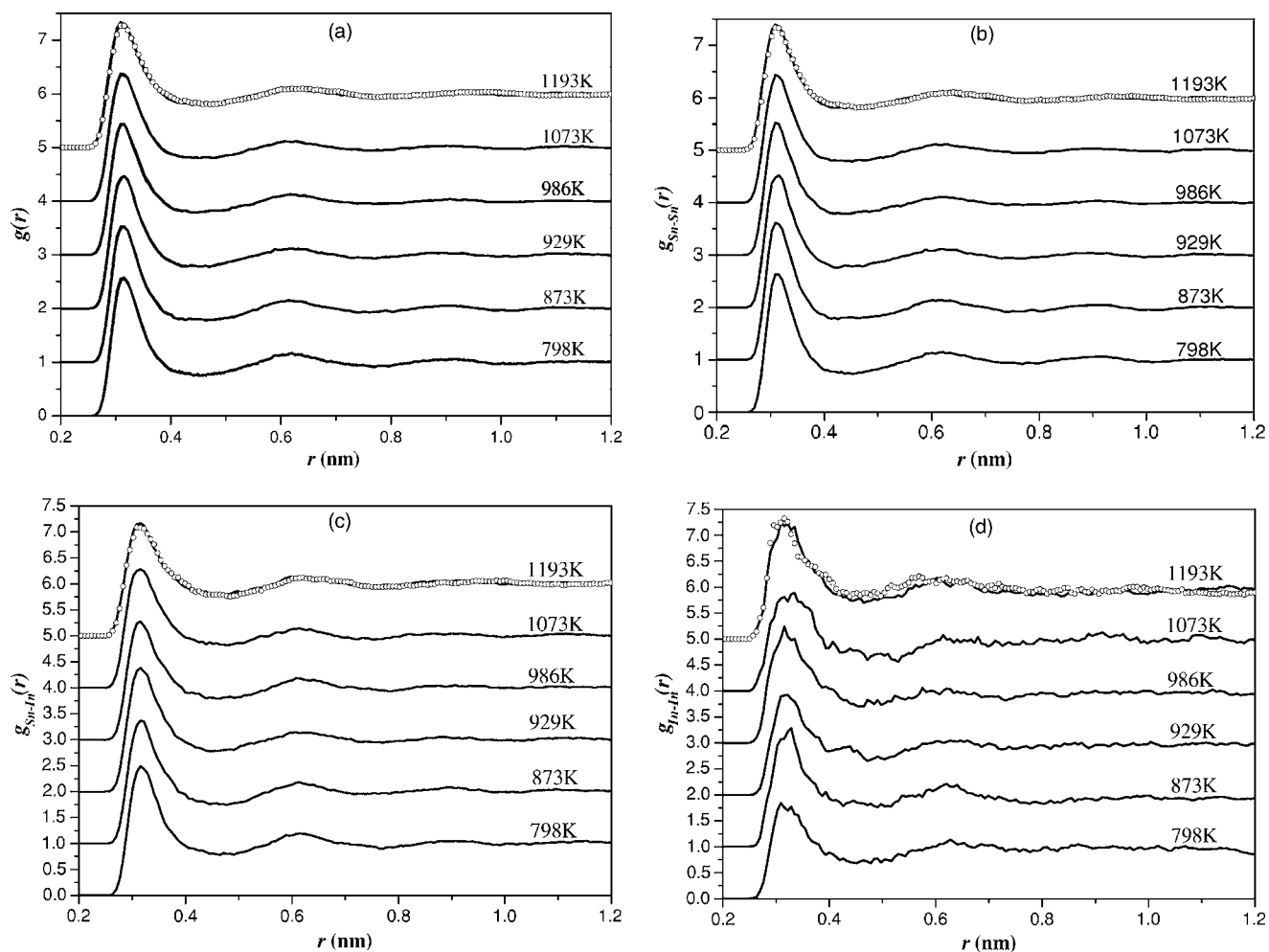


FIG. 2. Pair correlation functions of liquid $\text{In}_{20}\text{Sn}_{80}$ at different temperatures (open circles for a 120-atom system). (a) Total pair correlation function; (b) partial pair correlation function for Sn-Sn; (c) partial pair correlation function for Sn-In; and (d) partial pair correlation function for In-In.

temperature, no valley appears as in Fig. 1(c) of Ref. 17, but we can also find that it decreases more strongly in the low temperature range (from 798 to 986 K) than that at higher temperatures (from 986 to 1193 K), resulting in a noticeable bend between 929 and 986 K.

The structure factor, $S(Q)$, is also an important physical quantity. In a two-component alloy, the partial structure factor $S_{ij}(Q)$ can be obtained by the Fourier transformation of $g_{ij}(r)$,

$$S_{ij}(Q) = \delta_{ij} + 4\pi\rho_0 \int_0^\infty [g_{ij}(r) - 1] \frac{\sin(Qr)}{Qr} r^2 dr, \quad (5)$$

where i and j denote the two components of the binary alloy and ρ_0 is the average number density. The total structure factor $S(Q)$ is expressed as a linear combination of the three partial structure factor $S_{ij}(Q)$ normalized by the scattering lengths of the elements in the alloy,

$$S(Q) = \sum_{i=1}^2 \sum_{j=1}^2 \frac{c_i c_j b_i b_j}{(c_1 b_1 + c_2 b_2)^2} S_{ij}(Q), \quad (6)$$

where the neutron scattering lengths (b_{In} and b_{Sn}) are the same as defined in Eq. (2); c_i and c_j are their number concentrations, respectively. The total structure factors of liquid $\text{In}_{20}\text{Sn}_{80}$ alloy, shown in Fig. 4(a), were calculated at six different temperatures from 798 to 1193 K. It can be easily found that a shoulder is reproduced clearly in the high- Q side (around $Q=28 \text{ nm}^{-1}$) of the first peak. As mentioned in Ref. 22, due to the fragment of the tetrahedral unit remaining in liquid Sn, a shoulder appears at around $Q=28 \text{ nm}^{-1}$ in $S(Q)$ of liquid Sn. Thus, our present result confirms that the directional bonds of Sn atoms partially remain in liquid $\text{In}_{20}\text{Sn}_{80}$. The positions of the first peak and the second one seem not sensitive to the variation of temperature. Figure 4(b) plots the first-peak height of the structure factor as a function of temperature. As one can expect, the height of the first peak becomes lower and lower with the increase of temperature. However, in the low temperature region from 798 to 986 K,

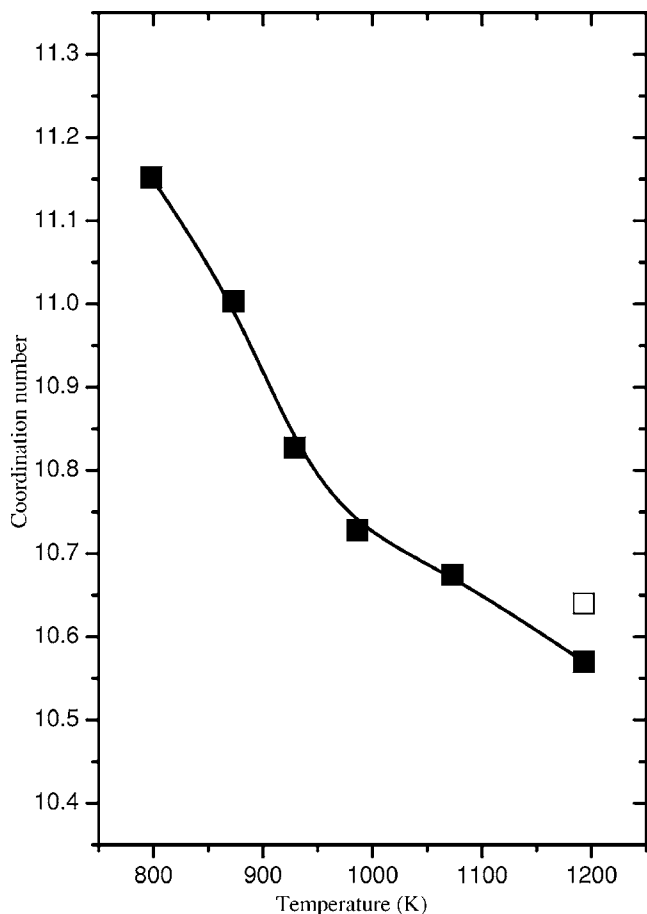


FIG. 3. Temperature dependence of the coordination numbers for a Sn atom (open square for a 120-atom system).

the peak height drops more sharply, compared to the high temperature region from 986 to 1193 K. In other words, there is a noticeable bend at around 986 K in the curve of peak-height versus temperature, indicating that an abnormal structural change may occur at around 986 K in a liquid $\text{In}_{20}\text{Sn}_{80}$ alloy. This is consistent with that found in the average coordination number of a Sn atom (as shown in Fig. 3).

The bond-angle distribution function $g_3(\theta)$, as one type of three-body distribution function, was calculated from the atomic configuration obtained by our simulations. The angle noted in $g_3(\theta)$ is formed by a pair of vectors drawn from a reference atom to any other two atoms within a sphere of a cutoff radius r_{cutoff} . Due to the directional bonds of Sn atoms partially remaining in liquid $\text{In}_{20}\text{Sn}_{80}$, it may provide more detailed information about the microscopic structure of liquid $\text{In}_{20}\text{Sn}_{80}$. Figure 5 gives the total bond-angle distribution function $g_3(\theta)$ of liquid $\text{In}_{20}\text{Sn}_{80}$ at six different temperatures with the bond length $r_{\text{cutoff}}=0.44$ nm. One can easily find that the bond-angle distribution function shows two peaks. For the first peak, its position is around 53° , invariable with the variation of temperature; but its height decreases with increasing temperature. The second peak is located around 102° , neither its position nor its height varies with increasing temperature. It is well known that when the interatomic interaction is isotropic and the atoms are packed in a closed-packed form, the $g_3(\theta)$ should show peaks around 60° and

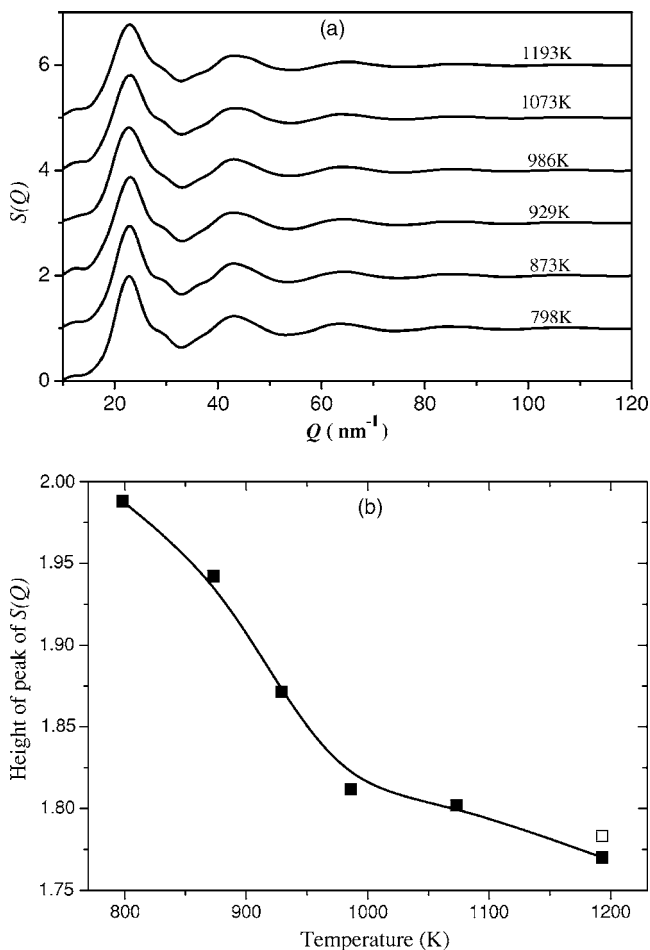


FIG. 4. (a) The total structure factor $S(Q)$ of the simulated liquid $\text{In}_{20}\text{Sn}_{80}$ at different temperatures; (b) temperature-dependent height of the first peak in $S(Q)$ of the simulated liquid $\text{In}_{20}\text{Sn}_{80}$ (open square for a 120-atom system).

120° . On the other hand, in the covalent bond crystal of diamond type with anisotropic interactions, it should show the tetrahedral bond angle of 109° . Therefore, here, the 53° peak indicates a feature of the typical simple liquid structure,

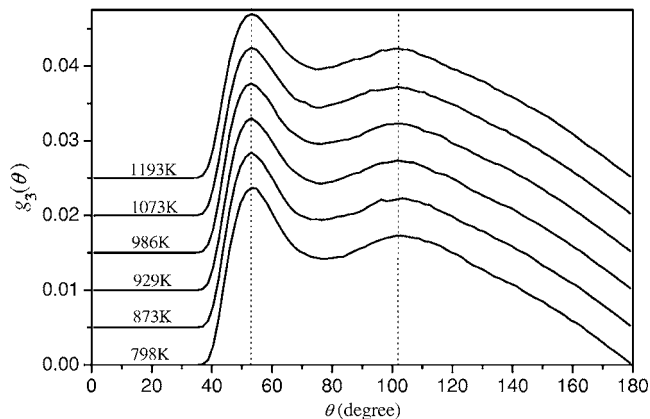


FIG. 5. Bond-angle distribution function of liquid $\text{In}_{20}\text{Sn}_{80}$ at different temperatures. The two dotted lines denote the location of two peaks.

but the second peak may be related to a complex local structure due to anisotropic interactions or an incomplete tetrahedral unit remaining in liquid $\text{In}_{20}\text{Sn}_{80}$.

To obtain more detailed information about the local atomic structure of the liquid $\text{In}_{20}\text{Sn}_{80}$ alloy, we use the pair analysis technique. The pair analysis technique, which was used by Blaisten-Barojas³² for decomposing the first two peaks of the pair correlation function and generalized by Honeycutt and Andersen,³³ has been widely used to monitor liquid, glass, and crystalline structures.³⁴ In this technique pairs of atoms can be classified by the relationship among their neighbors with four indices of integer. The first integer indicates whether the considered atomic pair is closer than a specified cutoff distance, chosen to be the nearest-neighbor distance determined by the first valley in the pair correlation function. Such atomic pairs are referred to as neighbors or, equivalently, are considered to form a bond. If the pair is bonded, the first integer is 1, or else, 2. The second integer is the common-neighbor number of the considered pair; the third represents the number of bonds among the common neighbors; the fourth is used to distinguish the atomic pair when the former three integers are not sufficient. A relative number of different types of pairs are normalized so that the total number of those pairs is unity. By counting all kinds of types of atom pairs, each of the various phases of a bulk system has its own signature that characterizes its local structure.³³ The 1421-type pair represents a fcc-like local structure, the 1422-type pair characterizes a hexagonal-close-packed-like (hcp-like) local structure, the 1441-type and 1661-type pairs characterize a body-centered-cubic-like (bcc-like) local structure, the 1551-type pair characterizes an icosahedronlike local structure, and the 1541-type and 1431-type pairs characterize the defect and disorder local structure.^{33–35} Note that, in our simulated liquid $\text{In}_{20}\text{Sn}_{80}$ the meaning of 1551-, 1541-, and 1431-type pairs may be a little different from that in simple liquid metal such as liquid Al and Cu, see the discussions below. Of the results obtained for different atomic bonded pairs, those that merit emphasis are summarized in Fig. 6. From this figure we can see that (i) With lowering temperature, a large increase occurs in the number of 1551-, 1541-, 1441-, and 1431-type pairs, whereas, a large decrease occurs in the number of 1201-, 1311-, 1321-, and 1422-type pairs. On the whole, those pairs pertaining to the relatively close-packed structure increase in the number with the decrease of temperature. (ii) In the high temperature region, the most prevalent atomic bonded pairs are the 1311 type, whereas in the low temperature region, the most prevalent atomic bonded pairs are the 1551 type. (iii) Compared with the high and low temperature region, in the middle temperature region (929–986 K), all pairs seem to increase or decrease much more strongly, thus, there seems to exist a steplike increase for 1551-, 1541-, 1441-, and 1431-type pairs and a steplike decrease for 1201-, 1311-, 1321-, and 1422-type pairs, implying that the liquid structure may change abnormally between 929 and 986 K.

In recent experiments, Zu *et al.*¹⁷ found in liquid $\text{In}_{20}\text{Sn}_{80}$ that, there is a clear peak at 973 K in the curve of internal friction versus temperature. Corresponding to the peak of the internal friction, a remarkable valley appears abnormally around 973 K for the mean nearest-neighbor distance and the

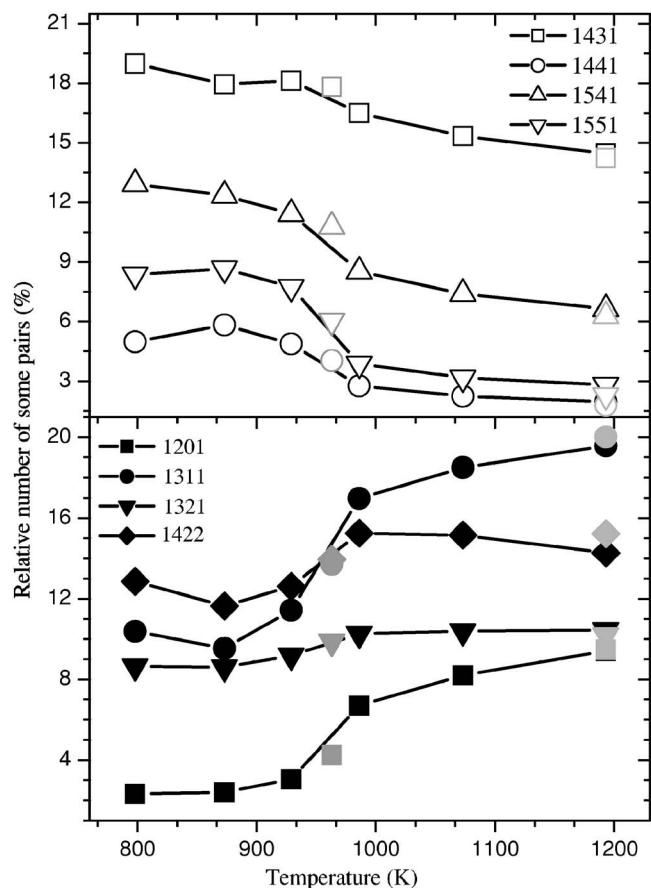


FIG. 6. Relative number of those main atomic bonded pairs as a function of temperature (see text for the data shown by gray symbols at 963 K and gray symbols at 1193 K for a 120-atom system).

coordination number, which vary only slightly with temperature before and after the valley, and the size of short-range orders and the ordering degree decreased abruptly at about 1030 K. This finding suggests a temperature-dependent discontinuous structural change could occur in liquid $\text{In}_{20}\text{Sn}_{80}$. Our present *ab initio* simulation shows that, the first-peak height of $S(Q)$ and the coordination number of a Sn atom decrease more sharply in a low-temperature region from 798 to 986 K than that in a high-temperature region from 986 to 1193 K; with the decrease of temperature there exist a steplike increase for 1551-, 1541-, 1441-, and 1431-type pairs and a steplike decrease for 1201-, 1311-, 1321-, and 1422-type pairs around 929–986 K. These results are in good agreement with the Zu's experimental observation, implying that an abnormal structural change may occur around 986 K in a liquid $\text{In}_{20}\text{Sn}_{80}$ alloy.

Recently, Tanaka¹⁴ presented a general view of a liquid-liquid phase transition on the basis of his proposed two-state model. The two-state model means that there always exist two competing orderings in any liquid: (i) density ordering leading to crystallization (long-range ordering) and (ii) bond ordering favoring a local symmetry (medium-range ordering) that is usually not consistent with the crystallographic symmetry. The former is characterized as the state of normal-liquid structures ($j=\rho$) and the latter is denoted as the state of locally favored structures ($j=S$). E_j , v_j , and g_j are the energy,

specific volume, and degeneracy of the j state, respectively. This model tells us that $E_S < E_\rho$ and $g_S \ll g_\rho$. The free energy is^{14,36}

$$f(S) = SE_S + (1 - S)E_\rho + [Sv_S + (1 - S)v_\rho]P + \kappa_B T \left[S \ln \frac{S}{g_S} + (1 - S) \ln \frac{1 - S}{g_\rho} \right] + JS(1 - S), \quad (7)$$

where T is the temperature and P is the pressure. J expresses the cooperativity of excitation and $J > 0$, which indicates the excitation of the same type of structures as its neighbor is energetically more favored than that of the different type. The local structures are “cooperatively” excited in the sea of the background structures (normal-liquid structures) and their number density increases upon cooling since $E_S < E_\rho$. The equilibrium value of S can be straightforwardly obtained, if the cooperativity term containing J in Eq. (7) is neglected, from the condition $\partial f / \partial S = 0$ as

$$\frac{S}{1 - S} = \frac{g_S}{g_\rho} \exp \beta [(E_\rho - E_S) - (v_S - v_\rho)P], \quad (8)$$

where $\beta = 1 / \kappa_B T$. As shown in Fig. 6, with lowering temperature a large increase occurs in the number of 1551-, 1541-, and 1431-type pairs, and there exists a steplike change in these local atomic structures around 929–986 K. In liquid $\text{In}_{20}\text{Sn}_{80}$, the existence of the short-range order with a tetrahedral unit is evidenced by the shoulder in the high wave

number side of the first peak of the structure factors shown in Fig. 4(a) and the peak located around 102° in the bond-angle distribution function shown in Fig. 5. The 1551-type pair, corresponding to two neighboring atoms with five common neighbors that form a pentagon of near-neighbor contacts, can be regarded as five tetrahedra organized around a common neighboring pair. Similarly, the 1541-type pair and the 1431-type pair can be regarded as five and four tetrahedra with some distortion. Therefore, the tetrahedral symmetry and the number of tetrahedra are enhanced through the increase in the abundance of 1551-, 1541-, and 1431-type pairs with lowering the temperature. Here, we analyze the temperature dependence of the relative number of 1551-type atomic bonding pairs, which is selected as an approximate estimation of the population of tetrahedral units (locally favored structures), namely, S in Eq. (8). We fit an exponential function like Eq. (8) to the temperature dependence of the relative number of 1551-type atomic bonding pairs. We find the exponential curve fitting is good, indicating that the structural transition (suggested by the steplike change in the local atomic structures shown in Fig. 6) is in agreement with the prediction of the two-state model without cooperativity. As is well known, it requires cooperativity that the first-order discontinuous liquid-liquid transition takes place. So, we would conclude that the presently observed abnormal structure-change in liquid $\text{In}_{20}\text{Sn}_{80}$ is not of first order. In order to corroborate this, we have performed another simulation of liquid $\text{In}_{20}\text{Sn}_{80}$ at 963 K. The obtained data of the

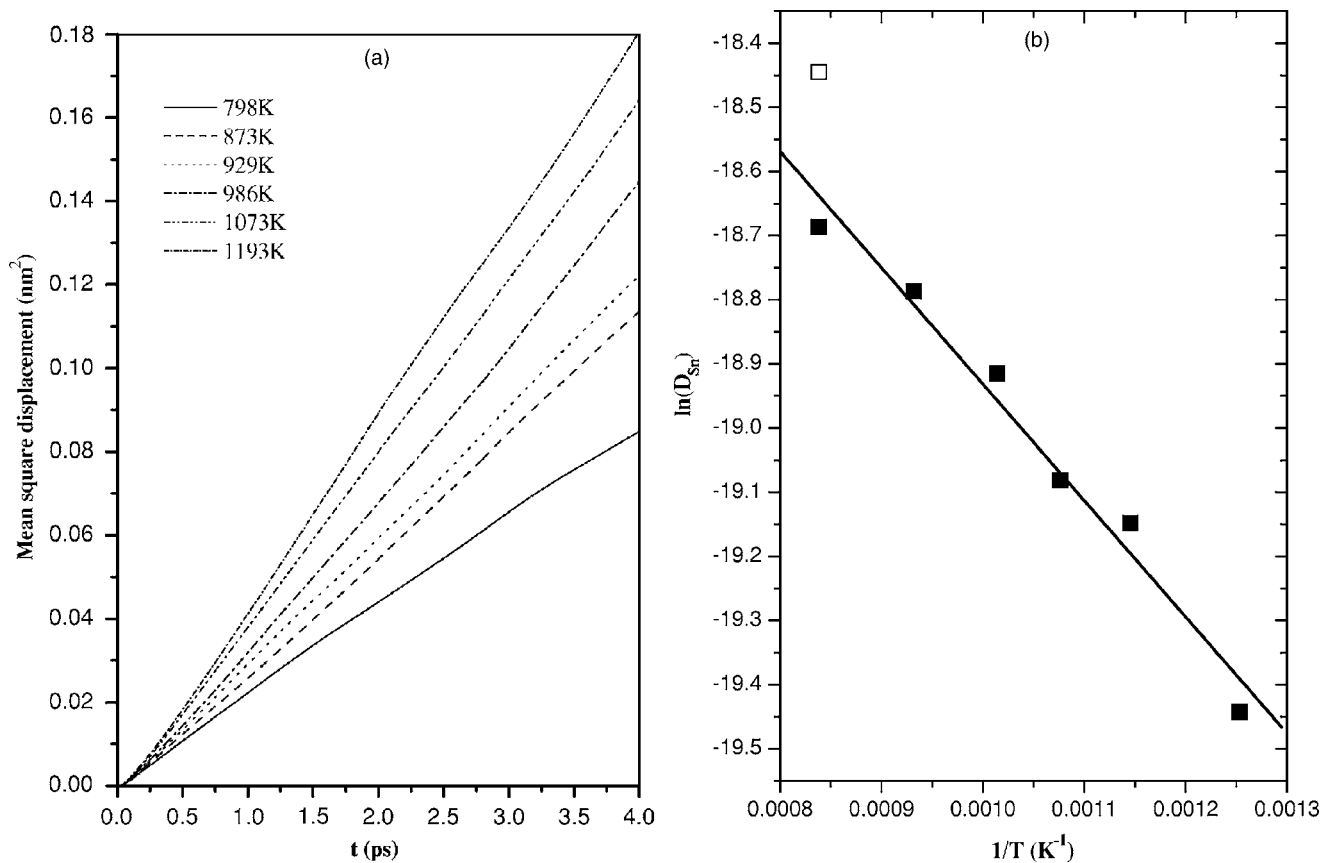


FIG. 7. (a) The variation of the mean square displacement (MSD) with time t , for a Sn atom in liquid $\text{In}_{20}\text{Sn}_{80}$; (b) the diffusion coefficient, D , of a Sn atom in liquid $\text{In}_{20}\text{Sn}_{80}$ as a function of temperature, T (open square for a 120-atoms system).

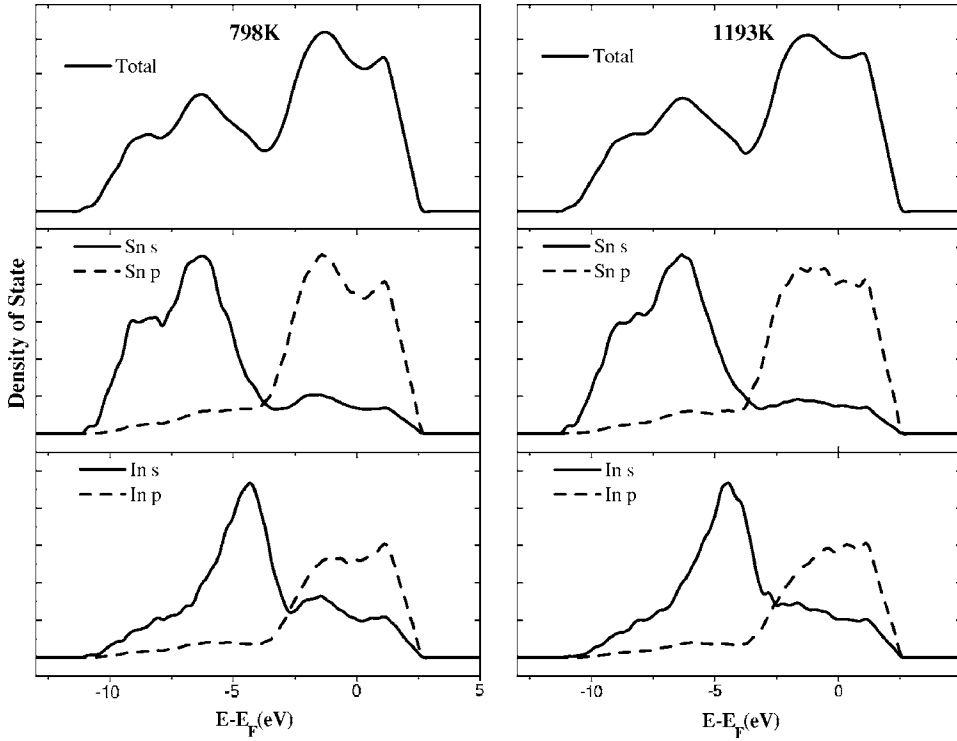


FIG. 8. The total and local electronic density of states for liquid $\text{In}_{20}\text{Sn}_{80}$ at 798 K (left panel) and 1193 K (right panel).

local atomic structures at 963 K are also presented in Fig. 6. From this figure, we can see that the change in local favored structure units around 929–986 K seems to be continuous, though the related atomic bonding pairs increase or decrease much more strongly in the temperature range 929–986 K than in both low and high temperature ranges. Therefore, it is not of first order that the abnormal structural change around 986 K occurs in a liquid $\text{In}_{20}\text{Sn}_{80}$ alloy.

During *ab initio* molecular dynamics simulations, the information of microscopic atomic motion can also be obtained. The diffusion behavior of Sn atoms in liquid $\text{In}_{20}\text{Sn}_{80}$ has been studied by calculating the time-dependent mean-square displacement (MSD), defined in the following way:

$$\langle \Delta r_{\alpha}(t)^2 \rangle = \frac{1}{N_{\alpha}} \left\langle \sum_{i=1}^{N_{\alpha}} |\vec{r}_{i\alpha}(t+t_0) - \vec{r}_{i\alpha}(t_0)|^2 \right\rangle, \quad (9)$$

where the summation goes over all N_{α} atoms of species α , \vec{r}_i is the coordinates of atom i , t_0 is an arbitrary origin of time, and the angular brackets denote an average over all possible time origins. As is well known, in liquid state, the MSD is linear with t in the limit of large time and the slope is proportional to the diffusion coefficient (D) according to the so-called Einstein relationship,

$$\langle \Delta r(t)^2 \rangle \rightarrow 6Dt + C, \quad (10)$$

where C is a constant. Figure 7(a) shows the MSD for Sn atoms at six different temperatures from 798 to 1193 K. The MSD always increases with time, this being consistent with the generalized Einstein model in which the atom in a cage, formed by its surrounding atoms, oscillates about a center which itself is undergoing Brownian motion. This also con-

firms that our sample is well in liquid state. According to Eq. (10), we can easily calculate the diffusion coefficients of Sn atom (D_{Sn}) at different temperatures. As shown in Fig. 7(b), the natural logarithm of D_{Sn} is plotted as a function of the reciprocal of temperature ($1/T$). The diffusion coefficients at 798 and 1073 K are in good agreement with the result of first-principles molecular dynamics simulation for pure liquid Sn.²² It can be approximately considered that the natural logarithm of D_{Sn} has a linear relationship with $1/T$, i.e., the temperature-dependent diffusion coefficient of Sn atom follows the Arrhenius relationship:

$$D = D_0 \exp(-E_D/k_B T), \quad (11)$$

where E_D is called the activation energy, D_0 is the preexponential factor, and k_B is the Boltzmann constant. By a linear fit of $\ln(D_{\text{Sn}})$ via $1/T$, the obtained E_D and D_0 are 0.16 eV and $3.68 \times 10^{-4} \text{ cm}^2 \text{ s}^{-1}$, respectively for a Sn atom.

The microscopic atomic structure is correlated with the electronic structure. So we have also studied the electronic density of state (DOS) and the local density of states (LDOS), i.e., the DOS for each atomic species is decomposed into angular-momentum-resolved contributions. By projecting all the wave functions in a sphere of radius R around atom i onto the spherical harmonic (l, m), we obtained the (l, m) angular momentum component of the atom i . For a binary system, there is no unambiguous way to define the value of the sphere radius R and several choices are possible. Here, we have used the covalent radius of atoms, $R_{\text{Sn}}=0.141 \text{ nm}$ and $R_{\text{In}}=0.144 \text{ nm}$. The calculated DOS and LDOS of liquid $\text{In}_{20}\text{Sn}_{80}$ at 798 K and 1193 K are represented in Fig. 8. We can see that there are four main peaks located near -8.5 , -6.3 , -1.3 , and $+1.0 \text{ eV}$ in DOS. From LDOS, we can see that the peaks near -8.5 eV and -6.3 eV

in DOS mainly result from an Sn (s) orbital and an In (s) orbital. The In-Sn bonds mainly result from the overlaps between the In (p) orbital and the Sn (p) orbital in which bonding and antibonding orbitals locate at -1.3 eV and $+1.0$ eV, respectively. As can also be seen, with the increase of the temperature to 1193 K, the gap at Fermi level becomes more shallow than that at 798 K, and the boundary between the bonding and antibonding states becomes more unclear.

IV. CONCLUSIONS

In summary, *ab initio* molecular dynamics simulations were performed for liquid $\text{In}_{20}\text{Sn}_{80}$ by using the cell size of 80 atoms. The structure properties of a liquid $\text{In}_{20}\text{Sn}_{80}$ alloy and its temperature dependence have been studied at constant pressure. The volume has an approximate linear relationship with temperature and the thermal expansion coefficient is $1.085 \times 10^{-4} \text{ K}^{-1}$ at 900 K, which is comparable to that of pure liquid Sn ($9.991 \times 10^{-5} \text{ K}^{-1}$ at 900 K). The pair correlation function, average coordination number, structure factor, and bond-angle distribution function at each temperature have been calculated. The calculated pair correlation function is in good agreement with experimental data. The existence of a shoulder in the high- Q side (around

$Q=28 \text{ nm}^{-1}$) of the first peak in the structure factor, along with the appearance of the peak at 102° in the bond angle distribution function, indicates that the residual directional bonds of Sn atoms exist in a liquid $\text{In}_{20}\text{Sn}_{80}$ alloy. There is a noticeable bend at around 986 K in the curves of the first-peak height of $S(Q)$ and the average coordination number of a Sn atom versus temperature, respectively, together with the behavior of the steplike change for some atomic bonded pairs, indicating that an abnormal structural change may occur around 986 K, which is qualitatively in agreement with experimental observation. However, the analysis based on the two-state model and the additional calculation at 963 K show that the change in local atomic structures is continuous, indicating that the abnormal structure change that happened in liquid $\text{In}_{20}\text{Sn}_{80}$ is not of first order.

ACKNOWLEDGMENTS

This work was supported by the National Natural Science Foundation of China (Grants Nos. 10174082 and 10374089) and the Knowledge Innovation Program of Chinese Academy of Sciences (Grant No. KJCX2-SW-W17), and by the Center for Computational Science, Hefei Institutes of Physical Sciences.

*Author to whom correspondence should be addressed. Email address: cslu@issp.ac.cn

- ¹O. Mishima and H. E. Stanley, *Nature (London)* **392**, 164 (1998).
- ²K. Koga, H. Tanaka, and X. C. Zeng, *Nature (London)* **408**, 564 (2000).
- ³A. K. Soper and M. A. Ricci, *Phys. Rev. Lett.* **84**, 2881 (2000).
- ⁴C. J. Roberts, A. Z. Panagiotopoulos, and P. G. Debenedetti, *Phys. Rev. Lett.* **77**, 4386 (2000).
- ⁵S. Harrington, R. Zhang, P. H. Poole, F. Sciortino, and H. E. Stanley, *Phys. Rev. Lett.* **78**, 2409 (1997).
- ⁶Y. Katayama, T. Mizutani, W. Utsumi, O. Shimomura, M. Yamakata, and K. Funakoshi, *Nature (London)* **403**, 170 (2000).
- ⁷G. Monaco, S. Falconi, W. A. Crichton, and M. Mezouar, *Phys. Rev. Lett.* **90**, 255701 (2003).
- ⁸N. Funamori and K. Tsuji, *Phys. Rev. Lett.* **88**, 255508 (2002).
- ⁹J. Y. Raty, J. P. Gaspard, T. Le. Bihan, M. Mezouar, and M. Bionducci, *J. Phys.: Condens. Matter* **11**, 10243 (1999).
- ¹⁰J. N. Glosli and F. H. Ree, *Phys. Rev. Lett.* **82**, 4659 (1999).
- ¹¹R. Winter, C. Szornel, W. C. Pilgrim, W. S. Howells, P. A. Egelstaff, and T. Bodensteiner, *J. Phys.: Condens. Matter* **2**, 8427 (1990), and references therein.
- ¹²S. Falconi, L. Lundegaard, C. Hejny, and M. McMahon, *Phys. Rev. Lett.* **94**, 125507 (2005).
- ¹³G. Franzese, G. Malescio, A. Skibinsky, S. V. Buldyrev, and H. E. Stanley, *Nature (London)* **409**, 692 (2001).
- ¹⁴H. Tanaka, *Phys. Rev. E* **62**, 6968 (2002).
- ¹⁵S. Aasland and P. F. McMillan, *Nature (London)* **369**, 633 (1994).
- ¹⁶C. J. Wu, J. N. Glosli, G. Galli, and F. H. Ree, *Phys. Rev. Lett.* **89**, 135701 (2002).
- ¹⁷F. Q. Zu, Z. G. Zhu, L. J. Guo, X. B. Qin, H. Yang, and W. J.

Shan, *Phys. Rev. Lett.* **89**, 125505 (2002).

- ¹⁸F. Q. Zu, L. J. Guo, Z. G. Zhu, and Y. Feng, *Chin. Phys. Lett.* **19**, 94 (2002); F. Q. Zu, Z. G. Zhu, L. J. Guo, B. Zhang, J. P. Shui, and C. S. Liu, *Phys. Rev. B* **64**, 180203(R) (2001); F. Q. Zu, Z. G. Zhu, B. Zhang, Y. Feng, and J. P. Shui, *J. Phys.: Condens. Matter* **13**, 11435 (2001).
- ¹⁹C. S. Liu, G. X. Li, Y. F. Liang, and A. Q. Wu, *Phys. Rev. B* **71**, 064204 (2005).
- ²⁰G. Kresse and J. Hafner, *Phys. Rev. B* **47**, R558 (1993); **48**, 13115 (1993); **49**, 14251 (1994).
- ²¹F. Kirchhoff, G. Kresse, and M. J. Gillan, *Phys. Rev. B* **57**, 10482 (1998).
- ²²T. Itami, S. Munejiri, T. Masaki, H. Aoki, Y. Ishii, T. Kamiyama, Y. Senda, F. Shimojo, and K. Hoshino, *Phys. Rev. B* **67**, 064201 (2003).
- ²³T. Gu, J. Qin, X. Bian, C. Xu, and Y. Qi, *Phys. Rev. B* **70**, 245214 (2004).
- ²⁴T. Gu, J. Qin, C. Xu, and X. Bian, *Phys. Rev. B* **70**, 144204 (2004).
- ²⁵M. Ji and X. G. Gong, *J. Phys.: Condens. Matter* **16**, 2507 (2004).
- ²⁶S. Y. Wang, C. Z. Wang, F. C. Chuang, J. R. Morris, and K. M. Ho, *J. Chem. Phys.* **122**, 034508 (2005).
- ²⁷P. E. Blochl, *Phys. Rev. B* **50**, 17953 (1994).
- ²⁸G. Kresse and D. Joubert, *Phys. Rev. B* **59**, 1758 (1999).
- ²⁹G. Kresse and J. Furthmuller, *Phys. Rev. B* **54**, 11169 (1996).
- ³⁰C. L. Yaws, *Chemical Properties Handbook* (McGraw-Hill, New York, 1999).
- ³¹J. Mesot, *Neutron News* **3**, 29 (1992).
- ³²E. Blaisten-Barojas, *Kinam* **6A**, 71 (1984).

- ³³J. D. Honeycutt and H. C. Andersen, *J. Phys. Chem.* **91**, 4950 (1987).
- ³⁴H. Jonsson and H. C. Andersen, *Phys. Rev. Lett.* **60**, 2295 (1988); C. S. Liu, J. Xia, Z. G. Zhu, and D. Y. Sun, *J. Chem. Phys.* **114**, 7506 (2001); C. S. Liu, Z. G. Zhu, J. Xia, and D. Y. Sun, *J. Phys.: Condens. Matter* **13**, 1873 (2001).
- ³⁵S. F. Tsay, *Phys. Rev. B* **48**, 5945 (1993); **50**, 103 (1994); S. F. Tsay and S. Wang, *ibid.* **50**, 108 (1994).
- ³⁶H. Tanaka, *J. Chem. Phys.* **112**, 799 (2000); *Phys. Rev. B* **66**, 064202 (2002).